Theoretical Analysis of the Dynamic Lateral Stability of a Paraglider

Jerzy Klimkowski & Wieslaw Lucjanek

Technical University of Warsaw, Faculty of Power and Aeronautic Engineering.

Presented at the 15th OSTIV Congress, Räyskälä, Finland (1976)

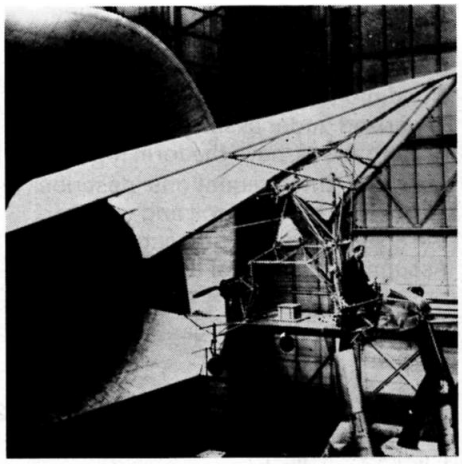

1. Powered parawing vehicle in wind tunnel [3].

Summary

A system of ordinary differential equations of a lateral motion of a flying vehicle, linearized and adopted to the case of a para-glider is presented. The stability of the system is analyzed by the method of small perturbations. As an example, the numerical calculations for the para-glider built by the student group from Technical University of Warsaw are performed. The influence of flight speed and altitude as well as pilot's position and vertical location relative to the wing is presented.

Aerodynamic Derivatives:

$$C_{lp}=\frac{2V}{b}\cdot\frac{\delta C_l}{\delta p},\qquad C_{np}=\frac{2V}{b}\cdot\frac{\delta C_n}{\delta p},\qquad C_{yp}=\frac{2V}{b}\cdot\frac{\delta C_y}{\delta p},$$

$$C_{lr}=\frac{2V}{b}\cdot\frac{\delta C_l}{\delta r},\qquad C_{nr}=\frac{2V}{b}\cdot\frac{\delta C_n}{\delta r}\qquad C_{yr}=\frac{2V}{b}\cdot\frac{\delta C_y}{\delta r},$$

$$C_{lv}=\delta C_l/\delta\bar{v},\qquad C_{nv}=\delta C_n/\delta\bar{v},\qquad C_{yv}=\delta C_y/\delta\bar{v}.$$

Symbols

A, B, C, D, E = coefficients of stability quartic (equation [3]),
b = wing span (m),
C_l = rolling moment coefficient (about x-axis),
C_n = yawing moment coefficient (about z-axis),
C_x = drag coefficient,
C_y = side-force coefficient (along y-axis),
C_z = lift coefficient,
g = gravity acceleration (9.81 m/s²),
H = flight altitude (m),
I_x, I_z, I_{xz} = moments of inertia and products moment relative to x and z axes (kg · m²),
$\bar{I}_x$, $\bar{I}_z$, $\bar{I}_{xz}$ = dimensionless I_x, I_z and $I_{xz}\cdot\bar{I}_x = 4\cdot g\cdot I_x/Q\cdot b^2$, etc.,
p = rolling velocity (about x-axis), (s^{-1}),
$\bar{p} = p\cdot t^*$ = dimensionless p,
Q = weight of a paraglider (N),
R = distance between center of gravity of a paraglider and aerodynamic center of a wing (canopy), (m),
$\bar{R} = R/b$ = dimensionless R,
r = yawing velocity (about z-axis), (s^{-1}),
$\bar{r} = r\cdot t^*$ = dimensionless r,
S = wing area (m²),
$T = -1n2\cdot t^*/\xi$ = time of a decrease of an amplitude to a half of its initial value (s),
t = time (s),
$t^* = Q/\varrho\cdot g\cdot S\cdot V$ = «aerodynamic» time (s),
$\bar{t} = t/t^*$ = dimensionless t,
V = speed of undisturbed flight (m/s),
v = sideslip velocity (along y-axis), (m/s),
$\bar{v} = v/V$ – dimensionless v,
W = descent velocity (m/s),
α = angle of attack of keel (deg),
η = imaginary part of λ,
$\lambda = \xi \pm \sqrt{-1}\cdot\eta$ = root of stability quartic (equation [3]),
$\mu = 2\cdot Q/\varrho\cdot b\cdot g\cdot S$ – relative density factor,
$\nu = \eta/2\cdot\pi\cdot t^*$ = frequency of oscillation (s^{-1}),
ξ = real part of λ,
ϱ = density of air (kg/m³),
φ = angle of bank (rotation about x-axis), (rad),
ψ = angle of yaw (rotation about z-axis), (rad),

Introduction

Ultralight wings, owing to their simple construction and to the possibility of deployment in the air, are in some respects similar to parachutes but are more controllable and make possible slower descent. The maximum lift to drag ratio of parawing vehicles is greater in magnitude by about an order as compared to parachutes. Owing to the advantages of the parawing vehicle, since the nineteen-fifties investigations were conducted into the use of parawings for soft landing systems for spacecraft [1]. Further research was directed into manned and remote-controlled vehicles [2], as well as to powered parawing vehicles (fig.1). Owing to the low cost and simplicity, parawing vehicles are built also by amateurs, and especially recently this type of aeronautical sport grows very rapidly.

In the paper, the dynamic lateral stability of a paraglider built by students of Warsaw Technical University is analyzed theoretically, Treating the results as representative for such vehicles, a comparison is made with the characteristics of a conventional aircraft.

Mathematical model and method of analysis.

The vehicle is considered as a rigid body and its motion is described in a rectangular right-handed set of axes Oxyz, with the origin at the center of gravity of the vehicle and the x and z axes in the plane of symmetry. In undisturbed flight the plane of symmetry is vertical, the

$$\left.\begin{aligned}
&\frac{d\bar{v}}{dt}-C_{yv}\cdot\bar{v}-\frac{C_{yp}}{\mu}\cdot\bar{p}+\left(1-\frac{C_{yr}}{\mu}\right)\cdot\bar{r}-\frac{C_z}{2}\cdot\varphi+\frac{C_x}{2}\cdot\psi=0,\\
&\frac{d\bar{p}}{d\bar{t}}-\frac{\bar{I}_{xz}}{\bar{I}_x}\cdot\frac{d\bar{r}}{d\bar{t}}-\frac{\mu}{\bar{I}_x}\cdot C_{lv}\cdot\bar{v}-\frac{C_{lp}}{\bar{I}_x}\cdot\bar{p}-\frac{C_{lr}}{\bar{I}_x}\cdot\bar{r}=0,\\
&-\frac{\bar{I}_{xz}}{\bar{I}_z}\cdot\frac{d\bar{p}}{d\bar{t}}+\frac{d\bar{r}}{d\bar{t}}-\frac{\mu}{\bar{I}_z}\cdot C_{nv}\cdot\bar{v}-\frac{C_{np}}{\bar{I}_z}\cdot\bar{p}-\frac{C_{nr}}{\bar{I}_z}\cdot\bar{r}=0.\\
&\bar{p}=\frac{d\varphi}{d\bar{t}},\\
&\bar{r}=\frac{d\psi}{d\bar{t}}.
\end{aligned}\right\}\qquad(1)$$

x-axis is directed forward and along the line of flight and the z-axis points downwards.
Nondimensional equations of motion, linearized under assumption of small perturbations, have the form [6]:
The first three equations describe respectively: sideslip, roll and yaw, and the last two are the kinematic relations.
Assuming the form of the solution:

$$\begin{bmatrix} \bar{v} \\ \bar{p} \\ \bar{r} \\ \varphi \\ \psi \end{bmatrix} = \begin{bmatrix} \bar{v}_o \\ \bar{p}_o \\ \bar{r}_o \\ \varphi_o \\ \psi_o \end{bmatrix} \cdot e^{\lambda \cdot t}. \qquad (2)$$

where subscripts "o" denote the constant initial values of functions at left-hand side of (2), the following characteristic equation of system (1) is obtained:

$$(A \cdot \lambda^4 + B \cdot \lambda^3 + C \cdot \lambda^2 + D \cdot \lambda + E) \cdot \lambda = O. \qquad (3)$$

where:

$$A = \frac{\bar{I}_{xz}^2}{\bar{I}_x \cdot \bar{I}_z} - 1,$$

$$B = \frac{C_{lp}}{\bar{I}_x} + \frac{C_{nr}}{\bar{I}_z} + \frac{\bar{I}_{xz}}{\bar{I}_x \cdot \bar{I}_z}\,(C_{lr} + C_{np}) + C_{yv}\left(1 - \frac{\bar{I}_{xz}^2}{\bar{I}_x \cdot \bar{I}_z}\right),$$

$$C = \frac{1}{\bar{I}_x}\,(C_{lv} \cdot C_{yp} - C_{lp} \cdot C_{yv}) + \frac{1}{\bar{I}_z}\,[C_{nv} \cdot (C_{yr} - \mu) - C_{nr} \cdot C_{yv}]$$

$$+ \frac{1}{\bar{I}_x \cdot \bar{I}_z}\,(C_{lr} \cdot C_{np} - C_{lp} \cdot C_{nr}) + \frac{\bar{I}_{xz}}{\bar{I}_x \cdot \bar{I}_z}\,[C_{lv} \cdot (C_{yr} - \mu)$$

$$+ C_{yp} \cdot C_{nv} - C_{yv} \cdot (C_{lr} + C_{np})],$$

$$D = \frac{1}{\bar{I}_x \cdot \bar{I}_z}\,[C_{yv} \cdot (C_{lr} \cdot C_{np} - C_{lp} \cdot C_{nr}) + C_{yp} \cdot (C_{lr} \cdot C_{nv} - C_{lv} \cdot C_{nr})$$

$$+ (C_{lp} \cdot C_{nv} - C_{lv} \cdot C_{np}) \cdot (\mu - C_{yr}) + \frac{\mu \cdot \bar{I}_{xz}}{2}\,(C_{nv} \cdot C_z - C_{lv} \cdot C_x)]$$

$$+ \frac{\mu}{2}\left(\frac{C_{lv}}{\bar{I}_x} \cdot C_z - \frac{C_{nv}}{\bar{I}_z} \cdot C_x\right),$$

$$E = \frac{\mu}{2 \cdot \bar{I}_x \cdot \bar{I}_z}\,[C_z \cdot (C_{lr} \cdot C_{nv} - C_{lv} \cdot C_{nr}) + C_x \cdot (C_{lp} \cdot C_{nv} - C_{lv} \cdot C_{np})].$$

Neglecting $\lambda_o = O$, equation (3) has four roots, generally complex:

$$\lambda_i = \xi_i \pm \sqrt{-1} \cdot \eta_i, \quad (i = 1..4). \qquad (4)$$

The motion of the vehicle is stable, if ξ_i values are negative. If $\eta_i \neq 0$, the motion is oscillatory with frequency ν.
For comparison of the modes of motion of the paraglider and the conventional aircraft, the ratio of initial values of functions at left-hand side of (2) (components of state-vector) has to be determined for all values of λ_i.

Numerical calculations
Stability equation (3) has been solved numerically for the particular vehicle [6], having the parawing shown schematically in fig. 2. The wing of weight 159 N has a skeleton made of duralumin tubes and is covered by nylon fabric. When stretched flat, the cover has the shape of two isosceles triangles hawing a common side 5.1 m long and apex angles of 45 deg. After deployment the cover has the shape approximately of two conical surfaces having a common generator, sweep angle of leading edge 50 deg, span 6.55 m and area 16.7 m² (aspect ratio 2.57). The pilot is represented by a cylinder of uniform density (ballast) of base diameter 0.224 m, height 1.7 m and weight 785 N. Therefore the total weight of the paraglider is 944 N and the wing loading 56.5 N/m².
The Center of gravity location of the skeleton, and the moments of inertia have been measured, but the contributions due to the deploye cover and the ballast they have been calculated. The center of gravity location of the paraglider and the moments of inertia are recalculated in Oxyz-axes system for each value of angle of attack of the keel and ballast position relative to the wing (requirement of longitudinal trim).
Aerodynamic forces are determined under assumption of stationary flow.
The Aerodynamic coefficients of the wing have been based on measurements described in [4], and the drag coefficients of the ballast are given in [5].
Aerodynamic derivatives relative to the system of wing axes are taken from [4] and for each case considered have been recalculated relative to the Oxyz-axes system.
Two variants of the pilot's position are analyzed:
1 = vertical and 2 = horizontal in the flight direction. For both variants calculations are performed for three configurations of vertical center-of-gravity location and for angle-of-attack of keel variation from 10 deg to 35 deg (speed variation from 21.2 m/s to 8.55 m/s for variant 1 and from 21.8 m/s to 8.57 m/s for variant 2). All calculations are performed for sea-level altitude. For variant 1 and angle-of-attack range between 25 deg and 35 deg, the influence of flight altitude from 0 to 1000 m is also investigated.

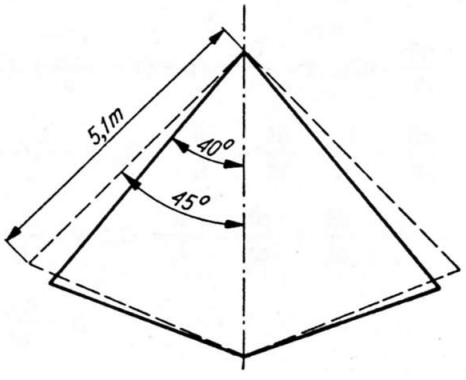

2. Geometric characteristics of a parawing. Dash lines show contours of flat fabric.

Results and discussion
Lift and drag coefficients of the paraglider versus angle-of-attack of keel for both variants are shown in fig. 3, and flight speed polars are presented in fig. 4. The position of the ballast has no

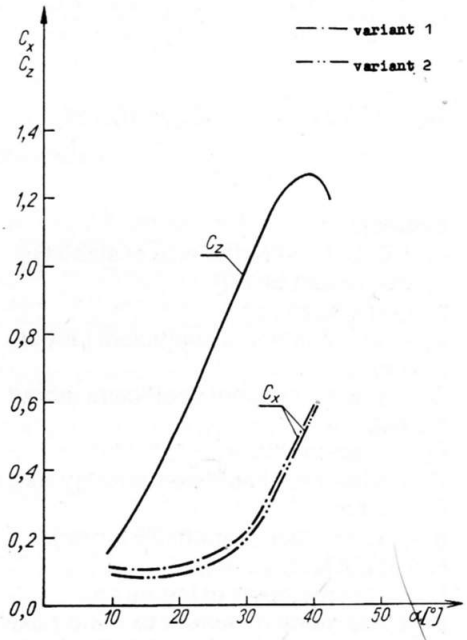

3. Lift and drag coefficients vs angle-of-attack of keel.

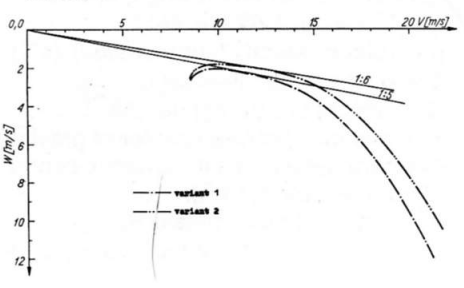

4. Flight speed polars of paraglider.

influence on lift, because only the drag of the payload is considered. Although the maximum lift-to-drag ratio seems to be optimistic, it should be noted that change of the pilot's position from horizontal to vertical may decrease this ratio by the order of unity.

In all cases investigated, two roots of equation (3) were complex with generally slightly negative real parts, and the two other roots were real and negative, but different in magnitude. For identification of the modes of disturbed lateral motion of the paraglider, the ratios of modula $\bar{v}_o$, $\bar{p}_o$, $\bar{r}_o$, φ_o and ψ_o to the value of $\sqrt{\bar{v}_o^2 + \bar{p}_o^2 + \bar{r}_o^2 + \varphi_o^2 + \psi_o^2}$ are calculated for each value of λ_i. Illustrative examples are presented in fig. 5.

It is shown, that the paraglider after disturbance performs the following asymmetric motions: corresponding to the pair of complex roots lightly damped lateral oscillations involving yawing, rolling and sideslipping, known as the Dutch roll, corresponding to the large negative root highly damped aperiodic rolling motion known as roll-subsidence mode and corresponding to the small negative root lightly damped aperiodic motion involving yawing and rolling, known as the spiral mode. Those results show, that although the paraglider configuration differs considerably from the conventional aeroplane (center-of-gravity location far below the wing, mass distribution mainly along the vertical axis, wing of untypical shape and absence of a fin), the lateral modes of vehicles of both configurations are similar.

Values of roots λ_i versus flight speed and vertical location of ballast for variant 1 are presented in fig. 6a, and corresponding dimensional values (T and v) in fig. 6b. In fig. 7 are presented values as in fig. 6 but for variant 2 and in fig. 8 the influence of flight altitude is shown.

For both variants the damping of the spiral mode slightly increases as the center-of-gravity is lowered and as flight speed increases. At the low speed the damping curves are not monotonic owing to the nonlinear relation between lift coefficient and angle-of-attack.

The damping of the roll-subsidence mode decreases as the center-of-gravity is lowered and as flight speed increases. Only for variant 1 and the uppermost payload location does the damping of this mode increase slightly with flight speed.

The frequency of the Dutch roll oscillation increases as the distance between ballast and wing decreases (moments of inertia decrease) and as flight speed increases (the "aerodynamic stiffness" increases), but the influence of the ballast location and flight speed on damping characteristics is different for the two variants. For variant 1 and uppermost ballast location, this mode is unstable at the higher flight speed.

Changing the center-of-gravity location involves changes in many factors, but probably the most important influence is the change of sign of aerodynamic derivatives C_{yr} and C_{jr} (see fig. 9).

The influence of flight altitude on the lateral stability is small (see fig. 8).

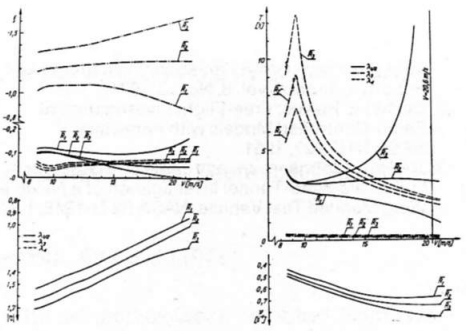

6. Values of λ_i (a), T and v (b) vs flight speed and vertical location of ballast. Variant 1, H = 0, $\bar{R}_1 = 0.230$, $\bar{R}_2 = 0.154$, $\bar{R}_3 = 0.076$.

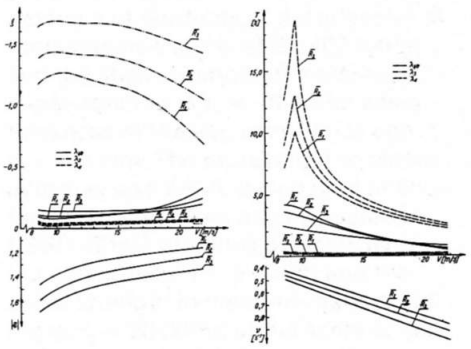

7. As in fig. 6 but for variant 2.

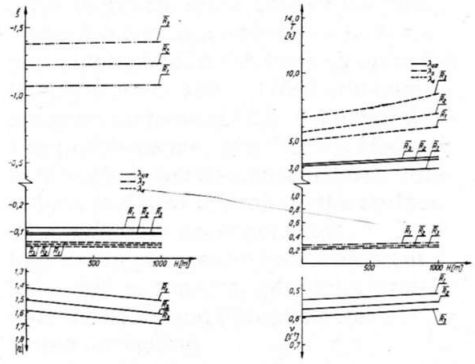

8. Values of λ_i (a), T and v (b) vs flight altitude and vertical location of ballast. Variant 1, V = 11 m/s, values of $\bar{R}$–s as in fig. 6.

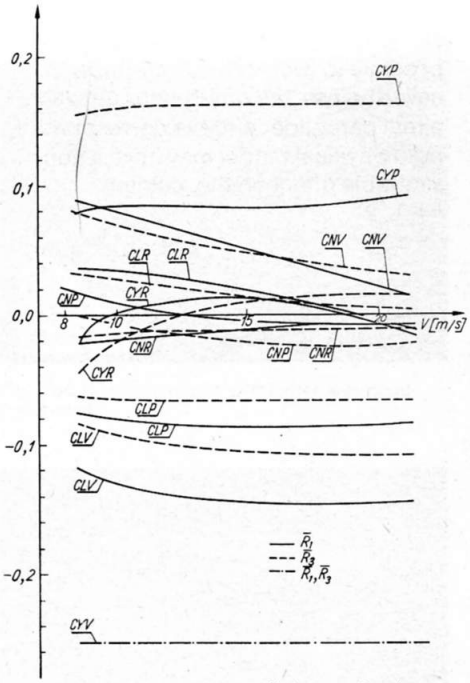

9. Aerodynamic derivatives vs flight speed and vertical location of ballast. Variant 1, H = 0, $\bar{R}_1 = 0.230$, $\bar{R}_3 = 0.076$. (CLP = C_{lp}, CYP = C_{yp}, etc.)

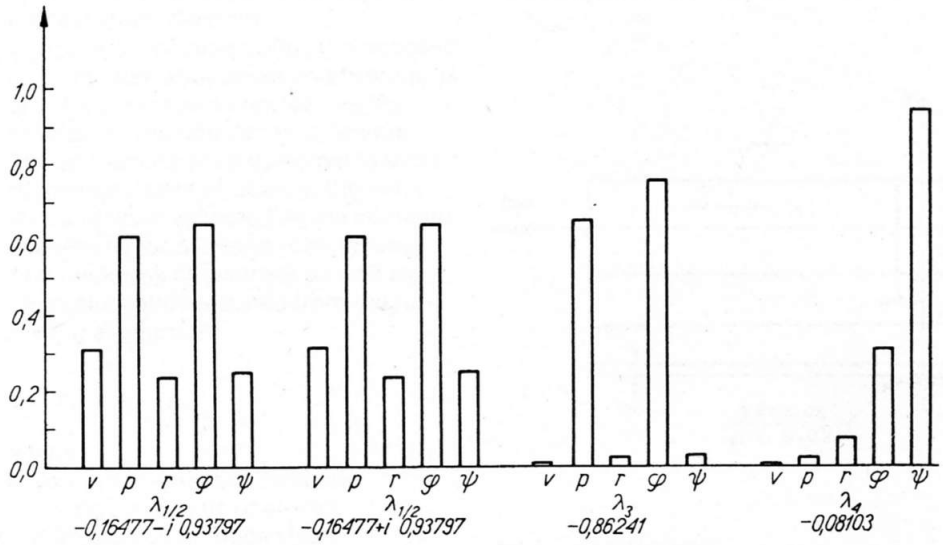

5. Ratios of modula of state vector components to the modulus of state vector. (i = $\sqrt{-1}$).

Concluding remarks

The results of a theoretical investigation of the dynamic lateral stability of a paraglider show, that the configuration considered is stable in the practical range of flight speed. In real flight conditions however, the aerodynamic characteristics of a wing may differ considerably from those taken in the calculations, because of the flexibility of the skeleton and fluttering of the aft portion of the fabric, especially at

higher flight speeds. By applying stringers sewn into the fabric, it is possible to reduce the fluttering; nevertheless, the differences between a real paraglider and the corresponding rigid physical model may have a considerable effect on the stability.

Bibliography

1. J. H. Moeller and E. M. Linhart: Parawing Technology for Spacecraft Land Landing a Progress Report. J. Aircraft, vol. 8, No. 12, 1971.
2. Donald E. Hewes: Free-Flight Investigation of Radio-Controlled Models with Parawings. NASA TN D-927, 1961.
3. Joseph L. Johnson, Jr., and James L. Hassell, Jr.: Full-Scale Wind-Tunnel Investigation of a Flexible-Wing Manned Test Vehicle. NASA TN D-1946, 1963.
4. Joseph R. Chambers and Peter C. Boisseau: A Theoretical Analysis of the Dynamic Lateral Stability and Control of a Parawing Vehicle. NASA TN D-3461, 1966.
5. Jerzy Bukowski: Mechanics of Fluids. Warsaw, 1970 (in Polish).
6. Jerzy Klimkowski: Dynamic Lateral Stability of a Paraglider. Thesis submitted to Faculty of Power and Aeronautic Engineering, Technical University of Warsaw, for the degree of Master of Science, 1976 (in Polish).